

Ionic Liquid High-Temperature Gas Sensor Array

Xiaoxia Jin,[†] Lei Yu,[†] Diego Garcia,[†] Rex X. Ren,[‡] and Xiangqun Zeng^{*,†}

Department of Chemistry, Oakland University, Rochester, Michigan 48309, and IL-TECH Inc., 69 Greenview Terrace, Middletown, Connecticut 06457

A novel sensor array using seven room-temperature ionic liquids (ILs) as sensing materials and a quartz crystal microbalance (QCM) as a transducer was developed for the detection of organic vapors at ambient and elevated temperatures. Ethanol, dichloromethane, benzene, and heptane were selected as representative gas analytes for various kinds of environmental pollutants and common industrial solvents. The QCM/IL sensors responded proportionately and reversibly to the organic vapor concentrations (i.e., ethanol, heptane, and benzene) in the gas phase from 0 to 100% saturation at room and elevated temperatures (e.g., 120 °C) but deviated from this linear relationship at high concentrations for dichloromethane, a highly volatile compound. Linear discriminant analysis was used to analyze the sensing patterns. Excellent classifications were obtained for both known and unknown concentrations of vapor samples. The correct classifications were 100% for known concentration samples and 96% for samples with unknown concentrations. Thermodynamics and ATR-FT-IR studies were conducted to understand specific molecular interactions, the strength of the interaction between ILs and organic vapors, and the degree of ordering that takes place upon dissolution of the vapors in ILs. The different response intensity of the QCM/IL sensors to the organic vapors depends on the different solubilities of organic vapors in ILs and varying molecular/ion interactions between each organic vapor and IL. The diverse set of IL studied showed selective responses due to structural differences. Therefore, a sensor array of ILs would be able to effectively differentiate different vapors in pattern recognitions, facilitating discrimination by their distinctive patterns in response to organic vapors in both room and high temperatures.

Chemical sensors are of increasing interest within the field of modern analytical chemistry. The key component of most chemical sensors is the recognition element. The recognition element interacts with the analyte to be detected, thereby encountering a characteristic change in one of its physical properties. Some examples of characteristic changes are mass, refractive index, light absorbance, and redox potentials to name a few. Although new and improved sensors will continue to be developed, the most

crucial need in any sensor is the recognition element.¹ Improvements in the affinity, specificity, and mass production of recognition elements usually dictate the success or failure of the detection technologies in both a technical and a commercial sense.

Among all available materials, biological recognition elements (e.g., antibodies, aptamers, enzymes, nucleic acids, and receptors) show excellent selectivity and sensitivity. However, biosensor devices often cannot be used for more than a few weeks or in harsh environments due to their limited stability. Inorganic materials (e.g., metal oxides and semiconductors) are commonly used in commercial sensors because of their durability and suitability for operation at elevated temperatures. However, they have limited specificity. Organic materials are receiving more attention because of the vast menu of physical and chemical properties they provide and their synthetic flexibility. However, most organic materials have the same problems as biological materials due to their limited stability, especially at high temperatures. For example, most polymer materials with low T_g are not stable at high temperatures and will eventually deteriorate, leading to the loss of activity. Metal oxides were used for high-temperature gas sensing based on resistance change upon vapor sorption.^{2–4} However, the dependency of the resistance on the vapor concentration is not linear, which reduces the accuracy of quantitative analysis.⁵ Room-temperature ionic liquids (ILs), a class of compounds containing organic cations and anions, seem to combine the advantages of the other aforementioned materials for chemical sensing and particularly for gas sensing. ILs have negligible vapor pressure and high thermal stability in air.⁶ These unique properties make them well suited for coatings and for the detection of flammable volatile organic compounds (VOCs), since ILs reduce the hazards associated with flash points and flammability. ILs are excellent solvents that can support many types of solvent–solute interactions (hydrogen bonding, π – π interactions, dipolar interactions, ionic interactions). Different interactions might be simultaneously present in an individual IL solution, and the resulting properties of an IL solution depend on which interactions are dominant. More importantly, the synthetic flexibility allows ILs

- (1) Iqbal, S. S.; Mayo, M. W.; Bruno, J. G.; Bronk, B. V.; Batt, C. A.; Chambers, J. P. *Biosen. Bioelectron.* **2000**, *15*, 549–578.
- (2) Dutta, P. K.; Ginwalla, A.; Hogg, B.; Patton, B. R.; Chwieroth, B.; Liang, Z.; Gouma, P.; Mills, M.; Akbar, S. J. *Phys. Chem. B* **1999**, *103*, 4412–4422.
- (3) Ikohura, K.; Watson, J. *The Stannic Oxide Gas Sensor*; CRC Press: Boca Raton, FL, 1994.
- (4) Zhu, Y.; Shi, J.; Zhang, Z.; Zhang, C.; Zhang, X. *Anal. Chem.* **2002**, *74*, 120–124.
- (5) Simon, U.; Sanders, D.; Jockel, J.; Heppel, C.; Brinz, T. J. *Comb. Chem.* **2002**, *4*, 511–515.
- (6) Zhang, Z.; Reddy, R. G. In *EPD congress 2002*; Taylor, P. R., Ed.; TMS: Warrendale PA, 2002; p 199.

* Corresponding author. Tel.: 248-370-2881. Fax: 248-370-2312. E-mail: zeng@oakland.edu.

[†] Oakland University.

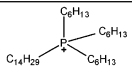
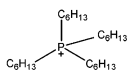
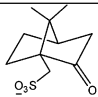
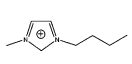
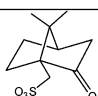
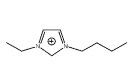
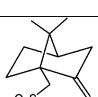
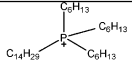
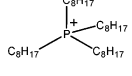
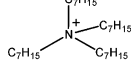
[‡] IL-TECH Inc.

to be tailored with a broad chemical diversity. One ion can be used to provide a function, and the second ion can provide a different, completely independent function.⁷ Functionalized ILs are being developed that act as solvents and as materials for particular applications.⁸ ILs' tremendous structural and chemical diversity and their remarkable thermal stability offer an opportunity to design a chemically selective IL sensor array and to explore their application for the detection and classification of gaseous analytes with pattern recognition at high temperature.

We report in this paper, for the first time, results of an IL sensor array for detection of selected flammable organic vapors (ethanol, dichloromethane, benzene, heptane) by a quartz crystal microbalance (QCM) transducer at high temperature (i.e., 120 °C). The selected gas analytes represent various environmental pollutants and common industrial solvents. Several criteria have been used for the IL selection. First, it is critical to have a pool of interfacial materials with as much chemical diversity as possible so that the arrays can respond to the largest possible cross section of analytes;⁹ i.e., their response patterns to the targets and interfering vapors must differ enough to achieve adequate selectivity. Second, they must have sufficient interactions with the target vapors to ensure adequate sensitivity. Finally, the material needs to be nonvolatile, stable at high temperatures, easy to synthesize to reduce the cost and has broad diversity to provide the flexibility of the sensor array.

The chemical selectivity of ILs to organic vapors depends on the interactions between ILs and the analytes. The interactions might include the following: dispersion, dipole induction, dipole orientation, or hydrogen-bonding interactions. The existence and the strength of the interactions are dictated by the structures of the ILs and the organic vapors. Therefore, varying the structures, and hence the properties, of the ILs can generate different types of interactions between the ILs and the organic vapors, thus enhancing the selectivity of the QCM/IL sensors. Table 1 lists two imidazolium ILs, four phosphonium ILs, and an ammonium IL selected as sensor array coating materials. A great deal of attention has been given to the imidazolium ILs, which consist of halogen-containing anions such as $[\text{AlCl}_4]^-$, $[\text{PF}_6]^-$, $[\text{BF}_4]^-$, $[\text{CF}_3\text{SO}_3]^-$, or $[\text{N}(\text{CF}_3\text{SO}_2)_2]^-$. For many technical applications, the presence of halogen atoms in the imidazolium IL may cause concern if the hydrolytic stability of the anion is poor (e.g., chloroaluminate and hexafluorophosphate systems) or if a thermal treatment of the IL is desired. As a result, imidazolium ILs with non-halogen anions have been selected. Other ILs selected are phosphonium or ammonium ILs with alkylsulfonate or alkylbenzenesulfonate anions. Their structures are distinctively different from those of the imidazolium ILs. They also possess high hydrolytic and thermal stability and acceptable viscosity. The ability to discriminate vapors depends on differences in the sorption isotherms among the IL sensor coatings in the array, which in turn depend on the volatility of each vapor and the strength of the interactions between the vapor and the IL coatings.

Table 1. Name and Structure of ILs Used

IL	Cation	Anion
$\text{P}_{66614}\text{MS}$		CH_3SO_3^-
P_{6666}CS		
BMICS		
BEICS		
$\text{P}_{66614}\text{DBS}$		$\text{C}_{12}\text{H}_{25}\text{phSO}_3^-$
$\text{P}_{8888}\text{DBS}$		$\text{C}_{12}\text{H}_{25}\text{phSO}_3^-$
$\text{N}_{7777}\text{DBS}$		$\text{C}_{12}\text{H}_{25}\text{phSO}_3^-$

To use the minimum number of sensors while obtaining the maximum information, we systematically vary the IL structure with the same or similar anions but different cations or vice versa so that the IL-coated sensors become an effective cross-respective sensor array. Specific functional groups selected in each IL should maximize particular interactions. This will ensure that one sensor array can identify more target analytes.

The QCM is an acoustic sensor using a piezoelectric crystal and has been extensively used as the transducer for gas sensing.¹⁰ When a thin and rigid film is strongly coupled to the resonator, the reversible oscillation–frequency shift (Δf) caused by the changes in mass (Δm) or modulus of the thin film can be quantitatively ruled by Sauerbrey's equation¹¹ ($\Delta f = -2\Delta m n f_0^2 / (A(\mu_q \rho_q)^{1/2})$, where n is the overtone number, f_0 is the eigenfrequency of a resonator, μ_q is the shear modulus of the quartz ($2.947 \times 10^{11} \text{ g/cm s}^2$), and ρ_q is the density of the quartz (2.648 g/cm^3)). In our report, the QCM/IL sensor array showed excellent identification and classification performances to the organic vapors with 100% analyte identification for known concentration samples and 96% for samples with unknown concentration. The interactions of each organic vapor with each individual IL coating were characterized by attenuated total reflectance (ATR) FT-IR. The ATR-FT-IR results show the specific molecular interactions between the different organic vapor and IL functional groups.

EXPERIMENTAL SECTION

Chemicals. Table 1 shows butylethylimidazolium camphor-sulfonate (BEICS), butylmethylimidazolium camphorsulfonate

(7) Rogers, R. D. *Chem. Eng. News* **2005**, 83 (31), 33–38.

(8) (a) Fei, Z.; Geldbach, T. J.; Zhao, D.; Dyson, P. J. *Chem.–Eur. J.* **2006**, 12, 2122–2130. (b) Lee, B. S.; Chi, Y. S.; Lee, J. K.; Cjoi, I. S.; Song, C. E.; Namgoong, S. K.; Lee, S. G. *J. Am. Chem. Soc.* **2004**, 126, 480–481. (c) Chi, Y. S.; Lee, J. K.; Lee, S. G.; Choi, I. S. *Langmuir* **2004**, 20, 3024–3027.

(9) (a) Albert, K. J.; Lewis, N. S.; Schauer, C. L.; Sotzing, G. A.; Stitzel, S. E.; Vaid, T. P.; Walt, D. R. *Chem. Rev.* **2000**, 100, 2595–2626. (b) Lewis, N. S. *Acc. Chem. Res.* **2004**, 37, 663–672.

(10) (a) Grate, J. W. *Chem. Rev.* **2000**, 100, 2627–2648. (b) Grate, J. W.; Martin, S. J.; Write, R. M. *Anal. Chem.* **1993**, 65, 987A. (c) Alder, J. F.; McCallum, J. J. *Analyst* **1983**, 108, 1169–1189. (d) King, W. H., Jr. *Anal. Chem.* **1964**, 36, 1735–1739.

(11) Sauerbrey, G. Z. *Phys.* **1959**, 155, 206–222.

(BMICS), tetrahexylphosphonium camphorsulfonate ($P_{6666}CS$), trihexyltetradecylphosphonium methanesulfonate ($P_{66614}MS$), trihexyltetradecylphosphonium dodecylbenzenesulfonate ($P_{66614}DBS$), tetraoctylphosphonium dodecylbenzenesulfonate ($P_{8888}DBS$), and tetraheptylammonium dodecylbenzenesulfonate ($N_{7777}DBS$) ILs, which have been synthesized by Dr. Rex Ren, IL-TECH Inc. (Middletown, CT) with over 98% purity. The preparation procedures of the ILs have been described in previous publications.¹² The organic compounds (benzene, dichloromethane, heptane, ethanol) are analytical reagents purchased from Aldrich and used as received. The saturated vapor pressure of the four organic vapors at room temperature are 100.84 mmHg for benzene, 45.67 mmHg for heptane, 59.02 mmHg for ethanol, and ~ 400.0 mmHg for dichloromethane.¹³

Testing of the QCM/IL Sensor Array. The aforementioned ILs were cast on both sides of the QCM (10 MHz, International Instruments, Oklahoma City, OK) from their ethanol solutions. Typical surface loading of ILs on QCM surfaces were in the 3–10 μg range that yields an IL film of tens to ~ 200 -nm thicknesses. Ultrathin films are preferred since they are more rigid and have little shear modulus change upon vapor sorption.¹⁴ The QCM/IL sensors were studied for their capability to identify and detect selected organic vapors at concentrations from 10 to 80% over a broad temperature range (25–200 $^{\circ}\text{C}$). A Maxtek RQCM instrument was used to measure the resonant frequency. Linear discriminant analysis (LDA) was done with a SYSTAT provided by Systat Software Inc. ATR-FT-IR spectra were recorded with a Bio-Rad 175c FT-IR spectrometer with a Specac ATR Kit mounted with a ZnSe crystal (Specac Inc., Woodstock, GA). A thin film of ILs (~ 5 –17 $\mu\text{g}/\text{cm}^2$) was cast on the crystal. An organic vapor was carried by a nitrogen flow into the ATR chamber. Pure N_2 was used to purge the chamber before and after the introduction of the organic vapors.

Instrument Setups. The flow rate of the N_2 carrier gas was controlled by digital mass-flow controllers (MKS Instruments Inc.). A low carrier gas flow rate, 30 mL/min, was used, since it ensures the saturation of carrier N_2 gas by the sample vapor after the carrier N_2 gas bubbles through the sample reservoir. The saturated N_2 flow was then diluted by a second N_2 flow, and the final concentration was calculated based on ideal gas laws. The diluted sample gas flowed through tubing, ~ 1 -m length, into the sensor chamber. The tubing and the sensor chamber were located in a GC oven, where the temperature was precisely controlled. The long pathway ensured homogeneous mixing of the sample vapor and the carrier gas and the establishment of temperature equilibrium. The saturated sample gas was considered to be 100%. Concentrations of diluted vapors in percentage were calculated proportionately.

RESULTS AND DISCUSSION

Characteristics of the QCM/IL Sensors. Sensitivity, selectivity, fast response time, reproducibility, and low detection limits are basic requirements for sensors. Sensitivity can be increased by increasing the thickness of the IL coatings. Figure 1 shows the frequency change as a function of IL thickness obtained from

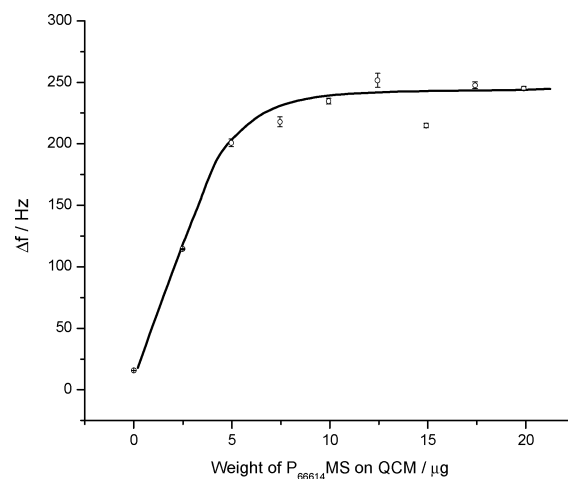


Figure 1. Frequency change vs IL film thickness of $P_{66614}MS$ (response to 80% (1470.4 g/m^3) CH_2Cl_2 at 120 $^{\circ}\text{C}$).

$P_{66614}MS$. When very thin films were used, the change of frequency increased linearly with the increase of the film thickness. However, response levels off when the thickness is larger than 200 nm. Each IL has its own linear range. In the following experiments, 3–10 μg of IL is used yielding an IL film of tens to ~ 200 -nm thickness. As two examples, at these thicknesses, the sensitivity of the $P_{6666}CS$ sensor to benzene is ~ 1.33 Hz/(g/m^3) and the $P_{66614}DBS$ sensor to ethanol is ~ 7.6 Hz/(g/m^3) at room temperature. The sensitivity will depend on the ILs used and the VOCs to be detected. The sensitivity also depends on the eigenfrequency of the QCM used. If the eigenfrequency of the QCM is increased from 10 MHz to 2 GHz, the sensitivity will theoretically increase 4×10^4 times.

Panels a and b in Figure 2 show representative sensorgrams of $P_{66614}DBS$ response to benzene vapor at various vapor pressures at 120 $^{\circ}\text{C}$ and to ethanol vapor at various temperatures at 80% concentration (i.e., 338.6 g/m^3 for benzene and 117.0 g/m^3 for ethanol, respectively). The sensorgrams show excellent reversibility of the adsorption/desorption processes. The excellent reversibility eliminates the need to purge the system to regenerate the sensing sites before each measurement, which allows a real-time monitoring. The response time and the sensitivity depend on the solubility equilibrium of organic vapors in IL thin films¹⁵ and the boiling point of the organic sample.¹⁶ When the flow rate was increased, the response time shortened, while the frequency change did not depend on the flow rate. Each time the sample channel was switched on or off, a constant frequency was established within minutes. In our experiment, the observed response time includes the time to reach equilibrium and the time to fill the sensing chamber. The analytical response time, which is much shorter, could not be obtained precisely. In our FT-IR experiments, a smaller chamber and a faster gas flow rate were used; the spectra showed full reversible responses in a couple of seconds, which indicated a very fast response. A fast response is a major advantage of IL coatings when compared to rubbery polymers and other solid coatings. This is because the diffusion

(12) (a) Ren, R. X.; Wu, J. X. *Org. Lett.* **2001**, 3, 3727–3728. (b) Ren, R. X.; Robertson, A. WO 0351894, 2003.

(13) Ohe, S. www.s-ohe.com.

(14) Grate, J. W.; Klusty, M. *Anal. Chem.* **1991**, 63, 1719–1727.

(15) Liang, C.; Yuan, C. Y.; Warmack, R. J.; Barnes, C. E.; Dai, S. *Anal. Chem.* **2002**, 74, 2172–2176.

(16) Grate, J. W.; Klusty, M.; McGill, R. A.; Abraham, M. H.; Whiting, G.; Andonian-Haftvan, J. *Anal. Chem.* **1992**, 64, 610–624.

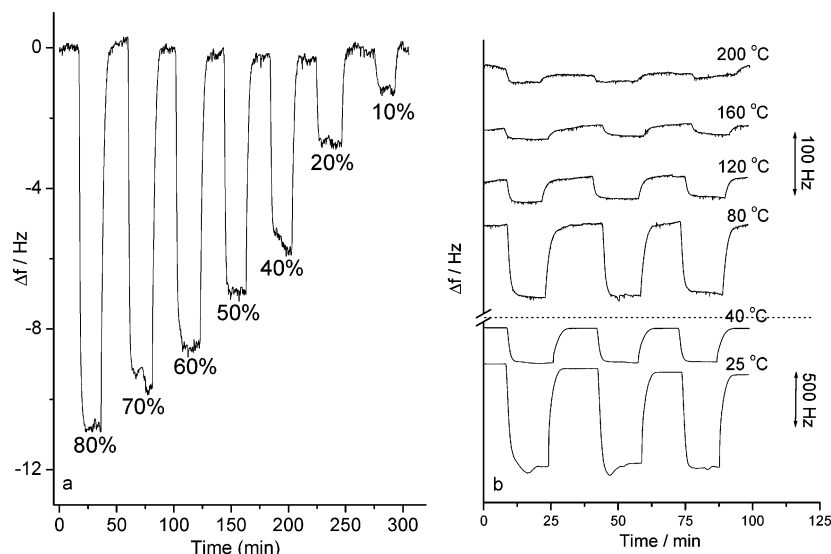


Figure 2. Sensorgrams of P₆₆₆₁₄DBS to benzene vapor at 120 °C (a) and to 80% (117.0 g/m³) ethanol at various temperatures (b).

of gas molecules in liquids is much faster than in polymers or solid materials. Similar sensorgrams have been observed for all other ILs and organic vapors tested (figures not shown) at both room and high temperatures. These results show that QCM/IL sensors have a fast and reversible response to various organic vapors at both room and high temperatures.

Figure 3 and Figure 4 summarize the results of frequency change as a function of the organic vapor concentrations for six ILs (the seventh was reported in an early work¹⁷). The QCM/IL sensors respond proportionately to the concentrations of benzene, heptane, and ethanol vapors over the full concentration range from zero to saturation at both room and elevated temperatures. When CH₂Cl₂, a highly volatile compound, was tested, the results deviated from the linear relationship when the concentration exceeded ~60% (1102.8 g/m³) of the saturation vapor pressure. The high vapor pressure of CH₂Cl₂ leads to the high molar fraction of CH₂Cl₂ in the IL phase that leads to its deviation from the ideal state. The different slopes in Figure 3 show the diverse sensitivity so that vapors can be discriminated by their differences in the sorption isotherms among the IL sensor coatings in the array. The differences in turn depend on the volatility of each vapor and the strength of the functional group interactions between the vapors and the IL coatings.

Pattern Recognition of Results from a QCM/IL Sensor Array. The above study demonstrates that a QCM/IL sensor has excellent sensitivity, linearity, stability, and reversibility and sufficient selectivity for organic vapor detection at both room and elevated temperatures. Classification or identification of different organic vapors could also be achieved by QCM/IL sensor arrays. The QCM/IL sensor responses in frequency change are normalized to the thickness of the IL films (in μg/cm²) and the concentration of vapor samples (in 100 g/m³). Sensing patterns from the above data are shown in Figure 5. Owing to the excellent linearity and great dynamic range shown in Figure 3, the patterns for each of the organic vapors were similar at a wide range of concentrations and temperatures studied (figures not shown). The lower the temperature is, the higher the intensity is. At lower concentrations the intensity was reduced.

Figure 6 illustrates the significance of the different patterns visually. The statistical analytical method LDA is employed. The LDA method converts the multivariates (Δf_{IL1} , Δf_{IL2} , ..., Δf_{IL7} , i.e., frequency changes from the QCM/IL sensor array) to canonical variances, so that the multidimensional data matrices (or the column chart patterns) are transformed into a more easily manageable and visually acceptable two-dimensional chart that contains the distinguishing signals of the original data as well.¹⁸ After the linear combination of the multivariates, the first two factors of the LDA results bear most of the distinguishable signals. The rest of the factors contain much less useful statistical differences. Therefore, two-dimensional LDA plots were drawn. In the resulting LDA plots, data points from one organic vapor sample should aggregate closely to form a cluster, while data points from different organic vapor samples might be separated. If the patterns can be recognized 100% correctly by the LDA method, the clusters of different organic vapor samples will not overlap with each other. Otherwise, the classification or identification of vapor by pattern recognition may not be achieved. In our work, we selected five replicate data from each organic vapor sample on each IL film. The thickness of the IL film and the concentration of the organic vapor are known. The LDA result in Figure 6 shows that the IL sensor array provides unique response patterns for each of the four vapors. The clusters from five replicate data sets are well separated from one another. There is no overlap of the data clusters in the canonical factor plots of the LDA results, which indicate excellent sample classification. The clusters of heptane and benzene are close since they are both nonpolar compounds. The “jackknifed” classification is 100% correct, Table 2. Therefore, given that the concentrations of the organic vapors in the gas (in w/v) are known, the classification or even identification of the organic vapors can be achieved by pattern recognition with LDA statistical methods using the experimental training set.

The LDA analysis was applied when the concentration was also a variable, to seven replicate data sets of the normalized data from various concentrations over the range of 20–80%. The results of the canonical plots are shown in Figure 7. From Figure 7, we see no overlap between the clusters of the four samples. The

(17) Yu, L.; Garcia, D.; Ren, R. X.; Zeng, X. *Chem. Commun.* **2005**, 2277–2279.

(18) Fisher, R. A. *Ann. Eugenics* **1936**, 7, 179–188.

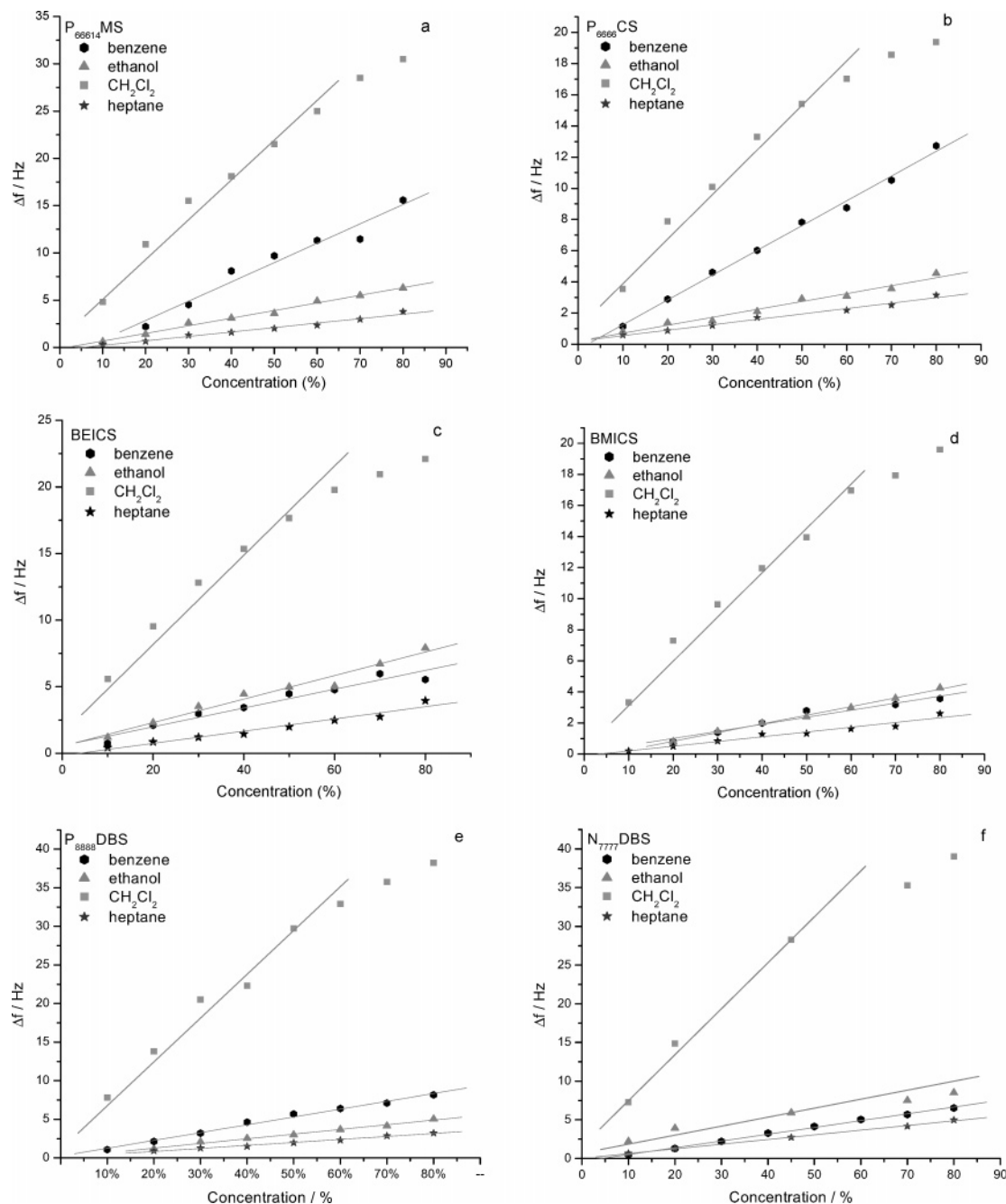


Figure 3. Δf as a function of the concentration of organic vapors for ILs P₆₆₆₁₄MS (a), P₆₆₆CS (b), BEICS (c), BMICS (d), P₈₈₈DBS (e), and N₇₇₇DBS (f) for four organic vapors at 120 °C. The straight lines represent the linear fit to the data with correlation coefficients of >0.972.

jackknifed classification results in 1 misclassification out of the total 28 cases, which yields a 96% correct identification, Table 3. This value is consistent with the LDA results from known concentration samples. Though the classification of an unknown concentration sample is not 100% correct, compared with other reported methods, the results are excellent.¹⁹ In our study, a seven-IL array was used for LDA analysis. Considering the diverse structures and properties of ILs, the ILs selected in this report may not represent the best set of IL array coatings. Once the selection of the particular set of ILs is optimized, excellent classification or identification of vapor analytes may be achieved by sensor array with a minimum number of IL coatings.

Thermodynamics of IL–Vapor Interactions. The high thermal stability of ILs makes them excellent materials for high-temperature applications. However, adsorption normally decreases with increasing temperature.²⁰ Figures 4 and 8 show the temperature dependence of the N₇₇₇DBS and P₆₆₆CS responses to various vapors. As expected from thermodynamic considerations, the frequency change (sensitivity) decreases exponentially with increasing temperature. As a result, piezoelectric sorption detectors become less sensitive and less selective as the temperature increases. Nonetheless, in our study, most ILs kept relatively

(19) Greene, N. T.; Morgan, S. L.; Shimizu, K. D. *Chem. Commun.* **2004**, 1172–1173.

(20) (a) Anthony, J. L.; Maginn, E. J.; Brennecke, J. F. *J. Phys. Chem. B* **2001**, 105, 10942–10949. (b) Anthony, J. L.; Maginn, E. J.; Brennecke, J. F. *J. Phys. Chem. B* **2002**, 106, 7315–7320. (c) Cadena, C.; Anthony, J. L.; Shah, J. K.; Morrow, T. I.; Brennecke, J. F.; Maginn, E. *J. Am. Chem. Soc.* **2004**, 126, 5300–5308.

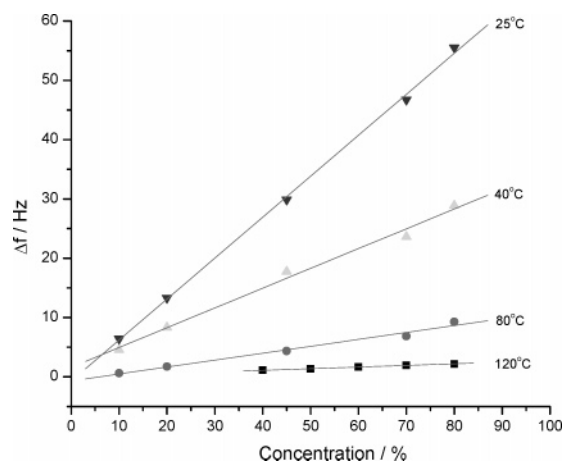


Figure 4. Δf vs concentration of heptane on $N_{777}DBS$ at 120, 80, 40, and 25 °C. The straight lines represent the linear fit to the data with correlation coefficients of >0.995 .

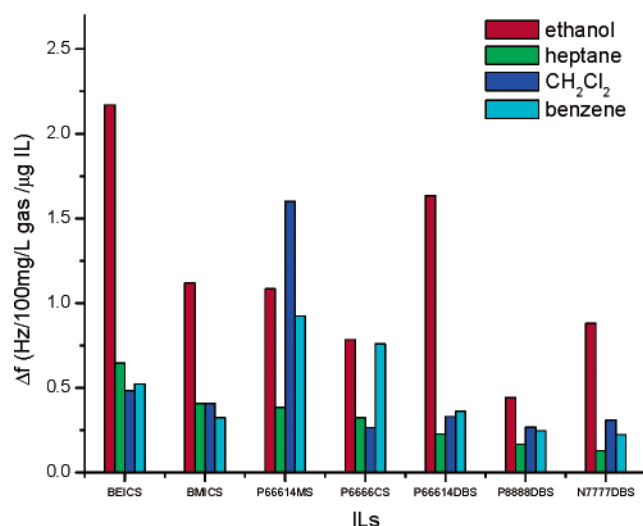


Figure 5. Signal patterns from 80% organic vapor samples at 120 °C. Responses are normalized to surface loading of ILs and concentration of vapors in gas.

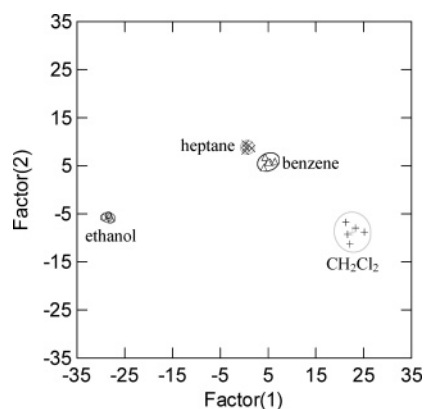


Figure 6. LDA canonical scores plots of the four vapors tested against ILs sensor array by 5 replicate data sets.

strong sensitivity even at 200 °C. We previously reported that the detection limit at 120 °C is a few grams per cubic meter.¹⁷ We also found the change of film modulus caused by the gas absorption on the IL film to be very small at high temperatures. Hence, at high temperature, the frequency changes were due

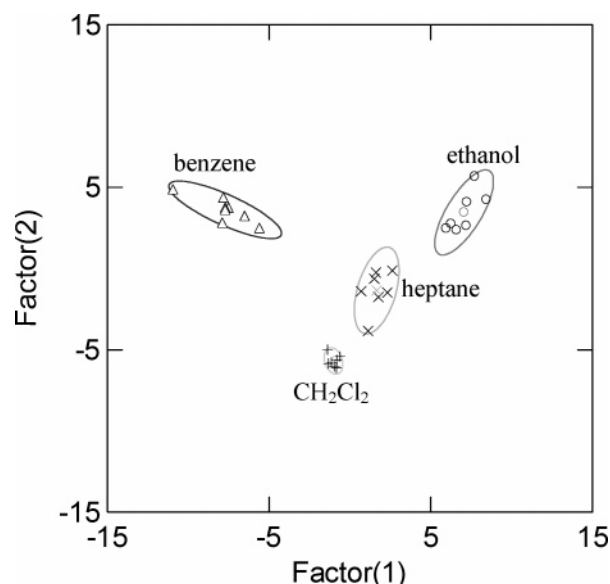


Figure 7. LDA canonical scores plot of the four vapors with different concentrations tested against ILs sensor array by 7 replicate data sets.

Table 2. Jackknifed Classification Matrix

label	ethanol	heptane	CH_2Cl_2	benzene	% correct
1	5	0	0	0	100
2	0	5	0	0	100
3	0	0	5	0	100
4	0	0	0	5	100
total	5	5	5	5	100

Table 3. Jackknifed Classification Matrix

label	ethanol	heptane	CH_2Cl_2	benzene	% correct
1	7	0	0	0	100
2	0	6	1	0	86
3	0	0	7	0	100
4	0	0	0	7	100
total	7	6	8	7	96

mainly to the mass loading in the IL film and the Sauerbrey equation relating frequency change to pure mass loading is valid. Consequently, the Henry constants can be measured with good accuracy at high temperature by QCM/IL sensors. The values of the Henry constants of the vapors in ILs at 120 °C were calculated according to the following equation

$$H_i(T) = \lim_{x_i \rightarrow 0} (P_i/x_i)$$

where P_i is the partial pressure of the samples in the gas phase, H_i is the Henry constant, and x_i is the molar fraction of the samples in the ILs. x_i was calculated from the Sauerbrey equation (for a 10-MHz crystal, the sensitivity is 1.02 ng/Hz).

Table 4 shows the values of the Henry constants of various vapors in ILs obtained from our experimental results. These results are consistent with data in Figure 3 that IL thin films have high sensitivity to polar analytes. CH_2Cl_2 shows strong signals

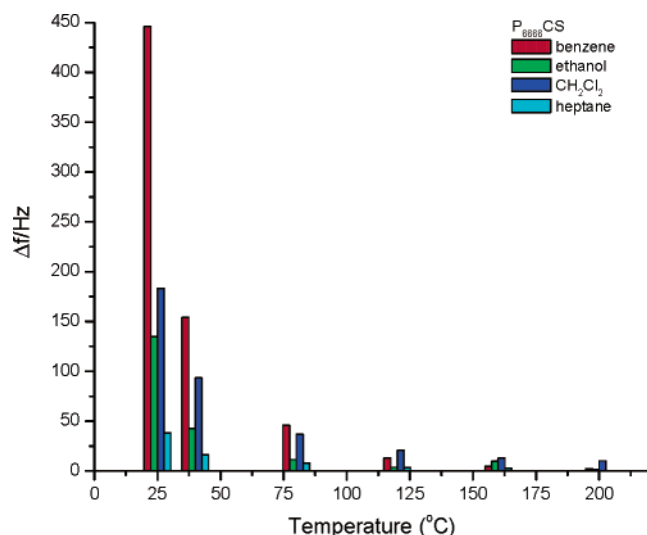


Figure 8. Δf vs T of $P_{666}CS$, 80% concentration.

Table 4. Experimentally Measured Values of Henry Constants^a

	ethanol	benzene	$CH_2Cl_2^b$	heptane
BEICS	0.33 ± 0.02	1.23 ± 0.13	1.04	1.25 ± 0.05
BMICS	0.58 ± 0.02	2.03 ± 0.10	1.11	1.67 ± 0.15
$P_{666}CS$	0.58 ± 0.04	0.55 ± 0.02	0.96	1.42 ± 0.10
$P_{66614}MS$	0.39 ± 0.01	0.43 ± 0.04	0.90	1.20 ± 0.05
$P_{66614}DBS$	0.19 ± 0.01	0.83 ± 0.04	0.61	1.26 ± 0.07
$P_{888}DBS$	0.72 ± 0.03	1.25 ± 0.05	1.02	1.88 ± 0.08
$N_{777}DBS$	0.47 ± 0.03	1.37 ± 0.03	0.76	1.15 ± 0.03

^a The unit of Henry constant is MPa. ^b Values of CH_2Cl_2 are calculated from the results of 10 and 20% concentrations, so there are no standard deviation values.

for all the QCM/IL sensors, while the Henry constants of CH_2Cl_2 are close to benzene and heptane. Therefore, the strong signals should be due to the high vapor pressure of CH_2Cl_2 . The difference of Henry constants provides the foundation for developing QCM/IL sensor arrays for pattern recognition.

From the data at different temperatures, adsorption enthalpy (ΔH_{ads}) and entropy (ΔS_{ads}) of the four organic vapors in four of the ILs are calculated using the van't Hoff equation,²⁰ considering that the molar fractions of the VOCs in the ILs are very small.

$$\Delta H_{ads} = -R(\partial \ln x_i / \partial T^{-1})_p$$

$$\Delta S_{ads} = -R(\partial \ln x_i / \partial \ln T)_p$$

where p is the partial pressure of gas, T is the temperature of the system, and x_i is the molar fraction of the gas dissolved in the ILs. The experimental data showed very good linear relationship of $\ln x_i$ versus $1/T$ and $\ln x_i$ versus $\ln T$. For example, $\ln x_i$ versus $1/T$ and $\ln x_i$ versus $\ln T$ curves from $P_{666}CS$ are shown in Figure 9.

Information about the strength of the interaction between ILs and gases can be provided by the enthalpy values, while the entropy values reflect the degree of ordering that takes place upon dissolution of the gases in ILs. The experimentally measured adsorption enthalpy and entropy of the organic vapors in the ILs

are shown in Tables 5 and 6. The last rows in Table 5 and Table 6 also list the ΔH_{vap} of the organic vapors at 25 °C and the ΔS_{vap} of the organic vapors at the boiling points, respectively. The differences between the ΔH_{ads} and ΔH_{vap} or ΔS_{ads} and ΔS_{vap} result from differences between the packing of vapor analyte in the IL and in their own liquid states owing to the differing structures, sizes, and shapes of the IL and differing IL–vapor intermolecular forces. These deviations can reveal something about the intermolecular interactions in ILs. For example, ΔH_{vap} of benzene and heptane are close to ΔH_{ads} of these two organic vapors in ILs (except $P_{666}CS$, probably caused by its bicyclic structured anion). These results indicate that the interactions between the benzene or heptane and ILs are close to benzene–benzene or heptane–heptane interactions. The interactions may be the result of the dipole induction interactions caused by the cations and anions of ILs. The strong dipole induction interactions of ILs and organic vapors ensure that IL sensors can detect nonpolar organic vapors with high sensitivity. ΔH_{vap} of CH_2Cl_2 is larger than ΔH_{ads} of CH_2Cl_2 in ILs, indicating that the interactions between CH_2Cl_2 molecules are stronger than the interaction between CH_2Cl_2 and ILs. ΔH_{ads} of ethanol are smaller than ΔH_{vap} of ethanol; hence, the hydrogen bonds between ethanol and ILs are not as strong as the hydrogen bonds among ethanol molecules. For the two polar molecules, ΔS_{ads} are smaller than their ΔS_{vap} at boiling point, which means that the ethanol and the CH_2Cl_2 molecules are less ordered in ILs than in their bulk liquids. The ΔS_{ads} of benzene are close to the ΔS_{vap} of benzene; therefore, the degree of ordering of benzene in ILs is close to that of benzene in bulk liquid. ΔS_{ads} of heptane is larger than ΔS_{vap} of heptane (data from $P_{666}CS$ is an exception; as mentioned above, this may be caused by the bicyclic structured anion of $P_{666}CS$). This may be due to the interactions of the alkyl chains of ILs causing the adsorbed heptane molecules to have a higher degree of ordering in ILs than in heptane liquid.

Characterization of the Interactions between ILs and Organic Vapors by ATR-FT-IR. A series of parameters have been used to quantify the interactions between commonly used organic solutes and the solvents.²² They are dispersion interactions parameter (or Ostwald solubility coefficient), polarizability, dipolarity, hydrogen bond basicity, and hydrogen bond acidity. Empirical values of these parameters for many organic compounds are available, while data for ILs are still not available. The values of these parameters depend on the structures of the cations and anions of ILs. For example, alkyl groups only contribute to the dispersion interactions and the strength of the interaction depends on the length and the configurations of the alkyl chains. The carbonyl group and the sulfonate group provide the possibility of hydrogen bonding that can strongly change the polarizability and the dipolarity of the ILs. The imidazolium may have π – π interactions with aromatic vapor analytes. In addition, the phosphonium, ammonium, and imidazolium have different ionic strengths. This will also affect the polarizability and the dipolarity of the ILs.

(21) *Knovel Critical Tables*; Knovel Corp.: Norwich, NY, 2003. www.knovel.com.

(22) (a) Grate, J. W.; Abraham, M. H. *Sens. Actuators, B* **1991**, 3, 85–111. (b) Anderson, J. L.; Armstrong, D. W.; Wei, G. T. *Anal. Chem.* **2006**, 78, 2893–2902. (c) Anderson, J. L.; Ding, J.; Welton, T.; Armstrong, D. W. *J. Am. Chem. Soc.* **2002**, 124, 14247–14254.

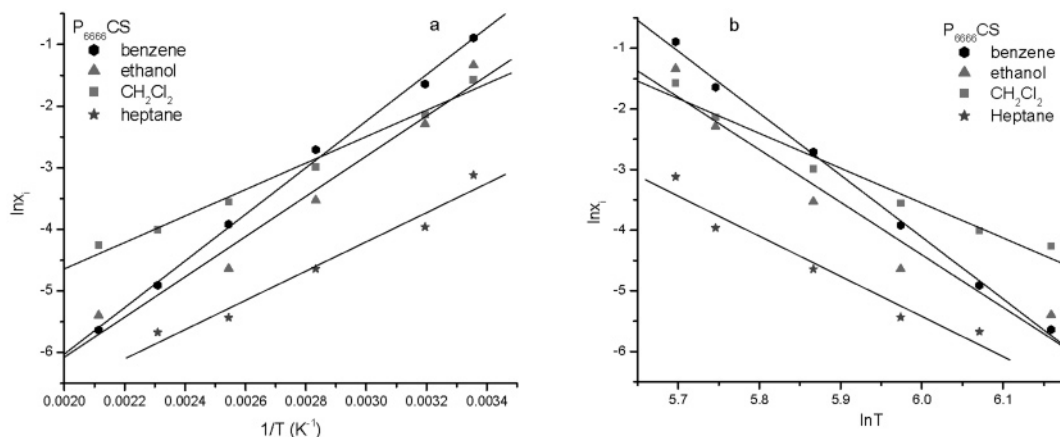


Figure 9. $\ln x_i$ vs $1/T$ (a) and $\ln x_i$ vs $\ln T$ (b) of the four organic vapors on adsorption $P_{666}CS$.

Table 5. Adsorption Enthalpy, ΔH_{ads} , and Vaporization Enthalpy, ΔH_{vap} , of Organic Vapors in ILs (kJ/mol) at 25 °C, 1 atm

	ethanol	benzene	CH_2Cl_2	heptane
BMICS	-25.2 ± 5.4	-32.0	-24.0 ± 0.6	-34.1 ± 3.2
$P_{666}CS$	-27.1 ± 2.8	-31.4 ± 0.9	-20.0 ± 1.5	-22.8 ± 6.5
$P_{666}MS$	-33.5 ± 3.1	-31.4 ± 1.0	-22.8 ± 0.8	-36.8 ± 1.3
$P_{666}DBS$	-26.5 ± 0.9	-36.1 ± 1.7	-23.8 ± 1.4	-37.5 ± 3.6
vaporization enthalpy ²¹ (ΔH_{vap})	-40.29	-34.46	-29.23	-36.49

Table 6. Adsorption Entropy, ΔS_{ads} , and Vaporization Entropy, ΔS_{vap} , of Organic Vapors in ILs (J/mol·K) at 25 °C, 1 atm

	ethanol	benzene	CH_2Cl_2	heptane
BMICS	71.7 ± 17.5	86.3	70.8 ± 3.9	100.1 ± 12.0
$P_{666}CS$	72.1 ± 10.4	84.8 ± 2.3	58.3 ± 5.7	69.3 ± 21.6
$P_{666}MS$	94.1 ± 8.9	88.5 ± 0.9	61.7 ± 1.0	108.4 ± 6.9
$P_{666}DBS$	71.1 ± 4.4	101.4 ± 5.4	63.7 ± 5.6	109.4 ± 13.2
vaporization entropy at bp ^a (ΔS_{vap})	112.1	87.1	90.7	85.4

^a Calculated from the vaporization enthalpy at boiling point (bp): $(\Delta S_{vap})_{bp} = -(\Delta H_{vap})_{bp}/T_{bp}$.

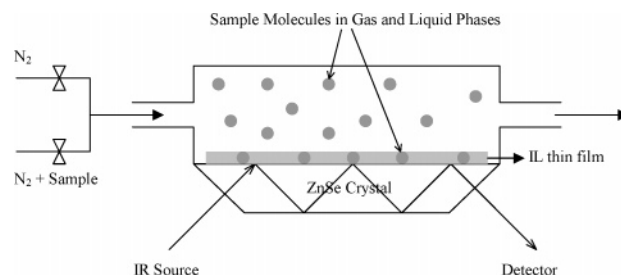


Figure 10. Flow cell setups for the ATR-FT-IR

when organic vapors are adsorbed on IL coatings. The spectra of heptane adsorption in each IL film are close to the sum of the spectrum of heptane and the spectra of each individual IL. However, peak shifts are observed when ethanol, benzene, and dichloromethane are adsorbed in each IL film, indicating specific molecularly interactions between a particular organic vapor and an IL. This strongly suggests that ILs could provide sensitivity and specificity for the organic vapor detection by sensor array.

Peak shifts caused by the specific interactions between the organic vapors and the ILs are observed when the organic vapors were adsorbed in the IL films. The extent of the shifts indicates the strength of the interactions. The stronger the interaction is, the larger the shift is. In the results for ethanol, three types of peak shifts were observed, related to the $-OH$ group of ethanol and the $-SO_3^-$ and $>C=O$ groups of the ILs. The $-SO_3^-$ group has two strong absorption peaks at about 1190–1200 and 1035–1040 cm^{-1} . The higher frequency arises from the asymmetric vibration and the lower frequency from the symmetric vibration. Adsorption of ethanol leads to ~ 15 –20- cm^{-1} red shift of the asymmetric vibration peak while the peak of the symmetric vibration overlaps with the ethanol peak at ~ 1050 cm^{-1} . The asymmetric vibration peak also becomes broader after ethanol adsorption. Polar solvents or hydrogen-bonding can cause a red shift of the $-SO_3^-$ absorption peaks.²³ Since the $-SO_3^-$ peak shift was absent when the other polar solvent CH_2Cl_2 interacts with the ILs, we rationalize that the $-SO_3^-$ group's asymmetric vibration peak shift is caused by the hydrogen bonding between the ethanol and the $-SO_3^-$ group. This interpretation is supported by the broad $-OH$ peak of ethanol centering at ~ 3360 cm^{-1} . This

ATR-FT-IR is a powerful method to elucidate the nature of chemical interactions at the gas/liquid interface. An ATR-FT-IR gas flow cell (Figure 10) is used to study the interactions between the vapor analytes and the IL thin films coated on the ZnSe crystal. ATR-FT-IR spectra of the four vapor analytes and seven ILs used are shown in Figure 11. Only the characteristic peaks of the vapor analytes and ILs are observed, indicating their high purity. The intensities of each peak for the organic vapors are very small due to the limited amount of the vapor adsorbed on the ZnSe crystal surface (Figure 11a). However, significant adsorption of organic vapors on the IL films is observed. The peak intensities increased 20–150 times compared to those on the bare ZnSe crystal (Figure 12). Additionally, identical ILs spectra can be recovered when pure N_2 is used to desorb the organic vapors. This result demonstrates the excellent reversibility of the adsorption and desorption processes of organic vapors in IL films. Also shown in Figure 12, characteristic peaks of organic vapors and ILs both were observed

(23) (a) Dolphin, D.; Wick, A. *Tabulation of Infrared Spectral Data*; John Wiley & Sons: New York, 1977. (b) Bellamy, L.J. *The Infrared Spectra of Complex Molecules*, 2nd ed.; Chapman and Hall: London, 1980.

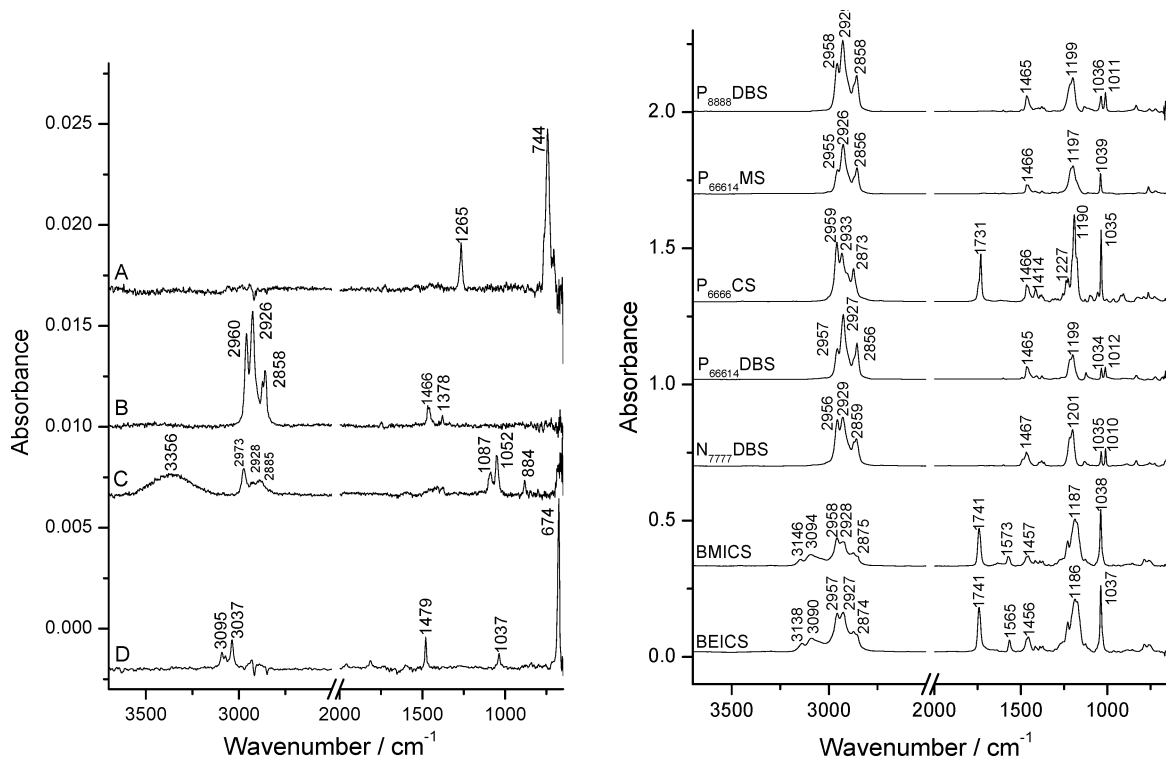


Figure 11. (a) ATR-FT-IR spectra of organic vapors on bare ZnSe crystal: CH_2Cl_2 (A), heptane (B), ethanol (C), and benzene (D) and (b) ATR-FT-IR spectra of ILs.

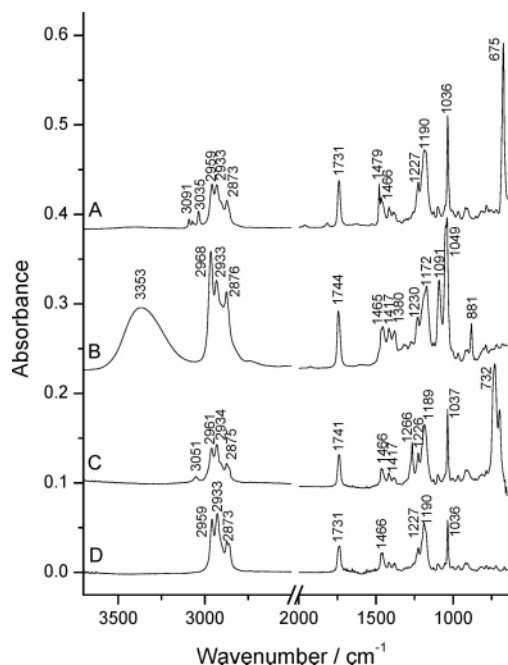


Figure 12. ATR-FT-IR spectra of P_{666}CS after absorption of benzene (A), ethanol (B), CH_2Cl_2 (C), and heptane (D).

change indicates that the $-\text{SO}_3^-$ group may interact with the $-\text{OH}$ group of ethanol and form a $-\text{O}-\text{H}\cdots\text{O}=\text{S}=\text{O}$ hydrogen bond. This interaction may also cause the $\text{C}-\text{OH}$ peak of ethanol at 884 cm^{-1} to shift to 881 cm^{-1} . The other peaks from ethanol did not shift after adsorption in ILs.

P_{666}CS , BEICS, and BMICS each have a camphorsulfonate anion, which contains a carbonyl group. The characteristic peak of the carbonyl group is at 1731 cm^{-1} for P_{666}CS and 1741 cm^{-1}

for BEICS and BMICS. After the adsorption of ethanol, the carbonyl peak blue shifted to 1744 cm^{-1} . This blue shift for the carbonyl group vibration was also observed when CH_2Cl_2 was adsorbed in P_{666}CS . In the CH_2Cl_2 case, the peak shifted from 1731 to 1741 cm^{-1} . The carbonyl group in both BEICS and BMICS shows a peak at 1741 cm^{-1} . However, no peak shift of the carbonyl group vibration in either BEICS or BMICS was observed upon adsorption of CH_2Cl_2 (spectra not shown) while it shifted to 1744 cm^{-1} when ethanol was adsorbed. The carbonyl peak shifting was also not observed when benzene and heptane were adsorbed in P_{666}CS , BEICS, and BMICS. This result implies that a polar solvent interacts with the carbonyl of the camphorsulfonate anion. The blue shift of the carbonyl peak may be caused by dipole–dipole interactions. It has been reported that polar solvents and hydrogen bonding will cause the carbonyl stretch vibration to red shift to lower frequency. However, we observed a high-frequency shifting in our spectra; the reason may be that the interactions of the solute with the sulfonate further affect the vibration of the carbonyl group.

In addition, CH_2Cl_2 showed two strong peaks at 1265 and 744 cm^{-1} on bare ZnSe crystal, which arise from the $-\text{CH}_2-$ wagging vibration and the aliphatic $\text{C}-\text{Cl}$ stretch vibration, respectively. After adsorption in the ILs, the peak at 744 cm^{-1} shifted to 732 – 738 cm^{-1} , while the peak at 1265 cm^{-1} did not change. The peak shifting may be caused by the interaction of the $-\text{Cl}$ with the H bonded on the α -carbons of the ILs.

In the benzene spectrum, peaks corresponding to the $\text{Ar}-\text{H}$ stretching vibration are located in the range of 3000 – 3100 cm^{-1} . On bare ZnSe, we observed three benzene peaks at 3095 , 3072 , and 3037 cm^{-1} . After adsorption in the phosphonium and ammonium ILs, the peak at 3095 cm^{-1} shifted slightly to 3091 cm^{-1} .

This change may be caused by the strong dipole–induced dipole interactions of benzene and the cations and anions of ILs. This interaction affected benzene's Ar–H stretching vibration but has no effect on ILs and other vibrations of benzene. In the imidazolium ILs, the peaks of benzene are overlapped with the peaks of imidazolium in the 3000–3100-cm⁻¹ range.

Heptane shows typical alkane peaks at 1378, 1466, 2858, 2926, and 2960 cm⁻¹. No peak shifts were observed for either heptane or ILs when heptane adsorbed into all ILs studied. Since all the ILs studied contain alkyl tails, the interaction may be simply the dispersion effects and the dipole induction interactions.

In summary, the ATR-FT-IR results showed that the interactions of organic vapors and ILs depend on their specific structures. The amount of organic vapors adsorbed in the IL films is dictated not only by the thickness of the IL films and the partial pressure of the vapors but also by the functional groups and chemical properties of the organic vapors and the ILs. The diverse set of ILs studied showed selective and unrelated responses due to their structural differences, which can be used to effectively spread different vapors out in feature space, facilitating discrimination for not only organic vapors but also other gas analytes.

CONCLUSIONS

Gas sensors are of increasing importance due to their potential applications in ambient air monitoring, occupational health and safety, biomedical diagnostics, industrial process control, and military and civilian counterterrorism. Extensive efforts have been made to develop new materials and transducers for gas sensing both at room and at high temperatures with particular emphasis on optimizing interface properties among the gas phase, the sensitive materials, and the transducer. In this report, we demonstrate that IL thin films perform well as sensor interfaces and provide additional control over selectivity and sensitivity when interacting with analytes in the gas phase. ILs possess negligible vapor pressure, high thermal stability, and structure diversity and prove to be excellent coating materials for chemical sensor arrays

in both room and high temperatures. Our study using seven ILs as sensing materials showed excellent classification results for both known and unknown concentration samples of organic vapors at room and high temperatures. The classification is 100% correct for known concentration samples and 96% correct for samples with unknown concentration. Both thermodynamic and ATR-FT-IR studies showed that the interactions of organic vapors and ILs depend on their specific structures. While there are ~300 organic solvents widely used in the chemical industry, there are potentially many more useful ILs that offer many options for chemical modifications and hence a huge flexibility in tailoring molecular recognition sites by controlled organic synthesis and surface design of ILs for use as chemical sensor arrays. In addition, QCM is one of the simplest transducers, which consist of coated crystals and a small resonating electronic circuit. Oscillator circuits are relatively simple and inexpensive to fabricate, which makes our sensor suitable for field instruments. This raises an exciting possibility of using QCM/IL arrays to assay different analytes in complex samples in a portable, fast, sensitive, reliable, and accurate manner.

ACKNOWLEDGMENT

This work is supported by Oakland University, partly by NIH (R33EB000672-02), and Michigan University Commercialization Initiative Challenge funds. We thank Dr. H. X. Qu in the Department of Mathematics and Statistics at Oakland University for his helpful discussion about data processing. We thank Dr. Mike Sevilla and Dr. John Seeley in the Department of Chemistry at Oakland University for their helpful discussion. We thank Dr. Dagmar Cronn in the Department of Chemistry at Oakland University for proofreading the manuscript.

Received for review May 11, 2006. Accepted July 28, 2006.

AC0608669